

Seasonal patterns in carbon dioxide in 15 mid-continent (USA) reservoirs

John R. Jones,^{1*} Daniel V. Obrecht,¹ Jennifer L. Graham,^{1,2} Michelle B. Balmer,³ Christopher T. Filstrup,³ and John A. Downing⁴

¹ School of Natural Resources, University of Missouri, Columbia, MO, USA

² US Geological Survey, Kansas Water Science Center, Lawrence, KS, USA

³ Department of Ecology, Evolution and Organismal Biology, Iowa State University, Ames, IA, USA

⁴ Minnesota Sea Grant & Large Lakes Observatory, University of Minnesota, Duluth, MN, USA

* Corresponding author: jonesj@missouri.edu

Received 25 February 2016; accepted 25 April 2016; published 26 April 2016

Abstract

Evidence suggests that lakes are important sites for atmospheric CO₂ exchange and so play a substantial role in the global carbon budget. Previous research has 2 weaknesses: (1) most data have been collected only during the open-water or summer seasons, and (2) data are concentrated principally on natural lakes in northern latitudes. Here, we report on the full annual cycle of atmospheric CO₂ exchanges of 15 oligotrophic to eutrophic reservoirs in the Glacial Till Plains of the United States. With one exception, these reservoirs showed an overall loss of CO₂ during the year, with most values within the lower range reported for temperate lakes. There was a strong cross-system seasonal pattern: an average of 70% of total annual CO₂ efflux occurred by the end of spring mixis; some 20% of annual flux was reabsorbed during summer stratification; and the remaining 50% of efflux was lost during autumnal mixing. Net annual flux was negatively correlated with depth and positively correlated with both water residence time and DOC, with the smallest annual CO₂ efflux measured in shallow fertile impoundments. Strong correlations yield relationships allowing regional up-scaling of CO₂ evasion. Understanding lacustrine CO₂ uptake and evasion requires seasonal analyses across the full range of lake trophic states and morphometric attributes.

Key words: atmospheric flux, carbon cycling, carbon dioxide, reservoirs

Introduction

The role of lakes in the global carbon budget is a topic of active research and debate. The partial pressure of carbon dioxide ($p\text{CO}_2$), the metric that determines the direction of carbon flux across the air–water interface, is regulated by factors related to water chemistry, productivity, lake morphology, and hydrology. Summaries on regional and global scales show a prevalence of CO₂ supersaturation in lakes and reservoirs, making them net emitters to the atmosphere (Cole et al. 1994, Duarte and Prairie 2005, Raymond et al. 2013). By contrast, recent findings show undersaturation is common during summer in eutrophic lakes located in the agricultural mid-continental USA

(Balmer and Downing 2011). Detailed carbon budgets for 5 hypereutrophic lakes and reservoirs in this same region indicate net atmospheric CO₂ uptake over an annual cycle is common, suggesting primary production can reduce CO₂ levels below atmospheric equilibrium (Pacheco et al. 2013). Missing is a broad seasonal perspective to quantify whether summer CO₂ uptake is balanced or exceeded by evasion in cooler seasons in reservoirs spanning the trophic gradient.

This research summarizes $p\text{CO}_2$ and carbon flux from 15 dimictic reservoirs in northern Missouri, located ~4° latitude south of the study sites of Balmer and Downing (2011) and Pacheco et al. (2013). Reservoirs were selected to represent the range of trophic conditions in the region (Table 1; Jones et al. 2008b). Our objectives were to measure $p\text{CO}_2$ and calculate gas exchange over an annual

Table 1. Mean concentrations of chlorophyll *a* (Chl-*a*), total phosphorus (TP), total nitrogen (TN), dissolved organic carbon (DOC), volatile suspended solids (VSS), and alkalinity (Alk), along with morphological and hydrological data for 15 Missouri reservoirs.

Lake	County	Chl- <i>a</i> ($\mu\text{g L}^{-1}$)	TP ($\mu\text{g L}^{-1}$)	TN ($\mu\text{g L}^{-1}$)	DOC (mg L^{-1})	Alk ($\text{mg L}^{-1} \text{CaCO}_3$)	Mean depth (m)	Area (ha)	Flushing Rate (times yr ⁻¹)
Nehai Tonkayea	Chariton	1.6	9	315	4.1	73	5.0	97	0.1
Forest	Adair	5.4	20	395	4.9	106	5.0	232	0.4
New Bethany	Harrison	5.6	18	650	6.0	89	4.6	30	0.3
Marie	Mercer	6.3	17	590	5.4	89	3.8	16	0.3
Brookfield	Linn	6.6	25	710	5.3	87	3.3	46	0.2
Hazel Creek	Adair	7.6	24	555	5.1	82	5.0	185	0.4
Marceline 2	Chariton	10.8	42	805	7.2	73	3.7	61	0.8
Green City	Sullivan	13.7	60	1035	7.5	63	1.5	21	1.2
Mozingo	Nodaway	14.0	30	925	6.4	107	5.7	408	0.3
Harrison Co.	Harrison	15.3	55	1090	9.1	93	3.7	113	1.2
Bilby Ranch	Nodaway	16.0	42	1070	7.6	120	4.1	45	0.5
Paho	Mercer	18.0	49	830	6.0	68	3.0	98	0.4
Nodaway	Nodaway	20.5	43	945	5.8	107	4.2	30	0.5
Marceline 1	Linn	26.0	100	1160	8.8	56	1.8	26	3.4
Sterling Price	Chariton	29.3	91	1510	8.1	67	1.6	10	2.0

cycle to determine seasonal patterns and potential relationships with limnological and physical characteristics of these reservoirs. Given the emphasis on summer conditions in the literature (Balmer and Downing 2011, Urabe et al. 2011, Trolle et al. 2012), we highlight CO₂ flux during summer stratification and throughout the open-water period.

Site description and methods

Study reservoirs were constructed in the Glacial Till Plains region of northern Missouri between 1950 and 1992. The range in size (10–408 ha), mean depth (1.6–5.7 m), flushing rate (0.1–3.4 times per year), and watershed crop cover (1–54%) represent regional reservoir conditions (Table 1; Jones et al. 2008a, 2008b).

Integrated photic zone samples were collected weekly between 12 January and 15 December 2004 (49 weeks). Climate in 2004 was characterized by protracted ice cover (until 8 March, week 9), a warmer and wetter spring than average (by 1.7 °C and 5.9 cm rainfall), and a cooler and wetter summer (by 2 °C and 6.6 cm rainfall). The El Niño-Southern Oscillation for this period was neutral.

During the first week, all reservoirs were sampled through the ice at a deepwater site near the dam; during weeks 2–8 the ice was unsafe, so most samples were collected from shallow locations or shoreline structures. Beginning week 9, all reservoirs were ice-free and sampled by boat at the deepwater site for the remainder of the study. Samples were analyzed for more than 60 water quality variables, including standard field measurements such as Secchi depth, temperature, and dissolved oxygen (DO)

profiles (model 85Yellow Springs International probe), plant nutrients measured as total nitrogen (TN) and total phosphorus (TP), chlorophyll (Chl-*a*), dissolved organic carbon (DOC), and zooplankton abundance. Field and laboratory methods are detailed in Jones et al. (2008b), and zooplankton were analyzed after Havel and Graham (2006). The majority of variables were measured weekly, consistent with the suggestion of Jonsson et al. (2007) for estimating CO₂ evasion.

Values of *p*CO₂ (μatm) and areal net atmospheric flux ($\text{g m}^{-2} \text{d}^{-1} \text{C}$) were calculated after Balmer and Downing (2011) using pH, alkalinity, and conductivity, as several others have done (Kling et al. 1992, Cole et al. 1994, Prairie et al. 2002). Equilibrium constants for various inorganic carbon species were calculated from the ionic strength (Butler 1992, Kling et al. 1992). Following Cole and Caraco (1998), potential areal net atmospheric CO₂ flux was calculated assuming an atmospheric value of 370 μatm. Wind speeds were normalized to 10 m above the water following the approach of Witter and Chelton (Brown 1979), using an average wind velocity of 3 m s⁻¹ (Cole and Caraco 1998). Alkalinity measurements were available for 180 samples (analyzed monthly), with the remaining values estimated based on regressions between alkalinity and conductivity ($r^2 = 0.70\text{--}0.94$). Where alkalinities were measured directly, calculations of *p*CO₂ based on measured alkalinity and alkalinity estimated from conductivity were not significantly different (paired samples *t*-test, $p > 0.05$).

Along with evaluating the whole dataset (annual, weeks 1–49), analyses were based on 3 seasonal subsets determined using temperature profiles to identify seasonal patterns: ice-out/spring mixing (weeks 1–17), summer

Table 2. Descriptive statistics for *p*CO₂ values (μatm) collected weekly from 15 Missouri reservoirs between 12 January and 15 December 2004 (49 weeks). Metrics include the mean, geometric mean, minimum value (Min), lower 10th and 25th percentile values, maximum value (Max), summer mean, and standard deviation for the period of collection.

Lake	Mean	Geometric mean	Min	10 th %	25 th %	Max	Summer mean	Standard Deviation
Nehai Tonkayea	410.5	384.2	195.3	240.3	381.4	1004.2	299.9	161.9
Forest	533.4	500.5	221.3	330.5	393.5	1084.4	417.6	193.3
New Bethany	458.9	431.7	169.9	274.8	345.5	916.3	348.5	162.3
Marie	400.6	349.6	159.8	175.6	224.1	1101.4	254.1	227.6
Brookfield	451.0	414.3	144.3	233.3	322.9	1133.5	304.9	195.2
Hazel Creek	437.2	396.5	151.0	209.1	294.6	1027.7	307.1	196.4
Marceline 2	471.5	426.7	122.9	230.7	328.4	1218.5	384.8	210.3
Green City	424.7	373.8	80.2	187.4	292.8	1498.6	388.1	236.7
Mozingo	508.7	467.2	104.3	215.7	383.4	915.0	352.0	188.5
Harrison Co.	532.0	442.5	65.9	161.3	304.1	1248.1	297.8	276.7
Bilby Ranch	402.8	309.3	70.2	110.4	142.1	1012.6	229.6	279.3
Paho	377.1	332.7	81.1	170.8	259.6	1197.7	276.5	207.2
Nodaway	420.8	368.9	90.9	135.3	253.8	897.6	254.7	203.1
Marceline 1	415.3	318.2	29.5	101.8	186.3	1185.3	261.0	272.9
Sterling Price	338.8	154.4	2.1	15.5	60.1	1193.0	83.0	317.2

stratification (weeks 18–35), and fall destratification (weeks 36–49). Carbon flux data are based on all 49 weeks of collection and expressed as annual flux; values are also presented for the open-water period (weeks 9–49) for general reference and to omit winter under-ice conditions, which can differ from other seasons (Ducharme-Riel et al. 2015). We calculated the potential areal CO₂ flux to or from the atmosphere by multiplying the calculated daily flux rate by the time interval between each weekly collection and by the number of weeks represented in each seasonal subset.

For visual presentation of cross-system seasonal patterns, *p*CO₂ and Chl-*a* data from the 15 individual reservoirs were normalized by subtracting the reservoir-specific mean from each observation and dividing by the reservoir-specific standard deviation for each metric; normalized values are represented using standard abbreviations with a subscripted N. Reservoir flushing rates were calculated after Jones et al. (2008a). Cross-system correlations are based on mean values (annual or seasonal) from the 15 reservoirs, and significance was set at $p \leq 0.01$. Regression models were interpreted using Akaike information criterion for small samples (AICc; Sugiura 1978). Correlation and regression analyses were performed using log10- and logit-transformed data.

Results

Mean Chl-*a* in these 15 impoundments ranged from 1.6 to 29.3 $\mu\text{g L}^{-1}$, representing oligotrophic to eutrophic conditions. Mean TN and TP also covered this trophic state range (Table 1; Jones et al. 2008b). About one-third

of the reservoirs were mesotrophic and 60% were eutrophic (Table 1). Mean depth, hydrology, and cropland in the watershed (a surrogate for nutrient loading) determine nutrient content in Missouri reservoirs (Jones et al. 2008a). A strong inverse correlation existed between mean TP and mean depth_(log) ($r = -0.89$) among the 15 study reservoirs, whereas the correlation with flushing rate_(log) was positive ($r = 0.94$). A 2-variable model (not shown) including flushing rate_(log) and percent cropland_(logit) explained 91% of cross-system variation in TP_(log) and 89% in TN_(log), consistent with previous findings for plains reservoirs (Jones et al. 2008a).

Metrics used to calculate *p*CO₂ were wide-ranging in the dataset, with pH varying from 7.6 to 10.0, alkalinity from 49 to 135 $\text{mg L}^{-1} \text{CaCO}_3$, and conductivity from 111 to 348 $\mu\text{S cm}^{-1}$. A strong negative correlation between *p*CO_{2(log)} and pH within each reservoir ($r \geq -0.98$) was expected given inorganic carbon chemistry in lake water and the use of pH in calculating *p*CO₂, making pH the best single predictor of *p*CO₂ in lakes (Lazzarino et al. 2009, Trolle et al. 2012, Knoll et al. 2013). Across all samples, a 2-variable model (not shown) including pH (negative coefficient) and conductivity_(log) (positive coefficient) accounted for 98% of variation in *p*CO_{2(log)}.

Values of *p*CO₂ varied from 2 to 1499 μatm (Table 2), with a mean of 439 μatm and a median of 408 μatm. These metrics of central tendency are about half the global estimate of Raymond et al. (2013; ~800 μatm) and about one-third the estimate for nontropical freshwater lakes, but some 20% larger than summer values measured in eutrophic Iowa lakes (median 322 μatm; Balmer and

Downing 2011). Overall, about half of the samples were supersaturated with CO₂, exceeding atmospheric CO₂ (370 μatm) by >10% (after Lazzarino et al. 2009).

Undersaturation and oversaturation of CO₂ was recorded in each reservoir during the study (Table 2). Among individual reservoirs, minimum values of *p*CO₂ varied by 2-orders of magnitude (2–221 μatm), geometric mean values by 3.2-fold (154–500 μatm), and maximum values by 2.4–4-fold atmospheric CO₂ (Table 2). The standard deviation of *p*CO₂ in these reservoirs was positively correlated with flushing rate_(log) ($r = 0.80$). Bottom quartile *p*CO₂ values, represented by the minimum and 10th and 25th percentile values in each reservoir, showed a cross-system increase with mean depth_(log) ($r = 0.72$ – 0.78), whereas values of *p*CO₂ decreased with mean concentrations of both plant nutrients and Chl-*a* ($r = -0.63$ to -0.96). Given these patterns, the lowest *p*CO₂ values were measured in shallow fertile impoundments.

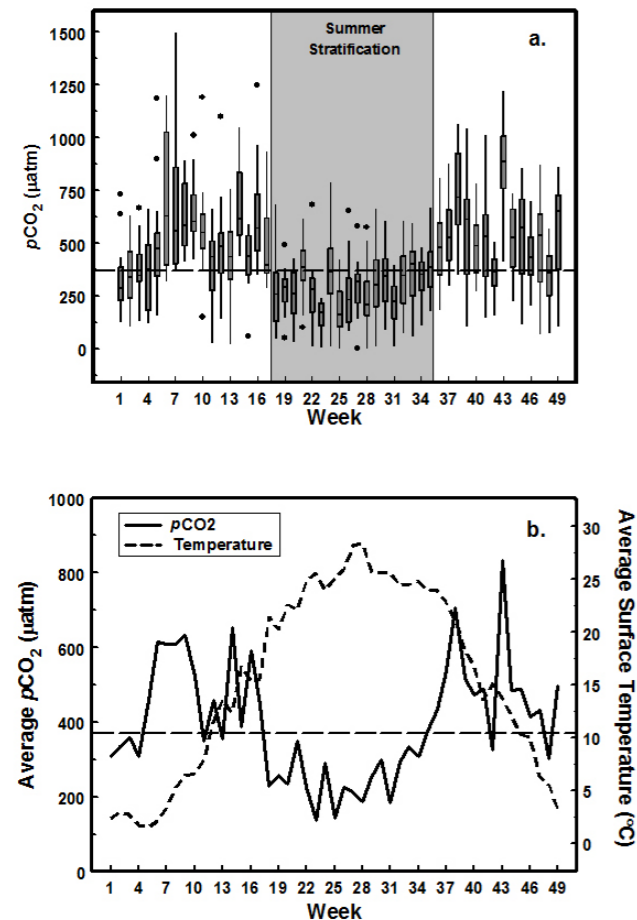


Fig. 1. Seasonal patterns of *p*CO₂ in 15 north Missouri reservoirs sampled over a 49 week period between 12 January and 15 December 2004. (a) Box plots of the data (measurements of values from all 15 reservoirs are shown by week of collection); (b) mean *p*CO₂ and mean surface temperature from the 15 reservoirs over the period of study. Horizontal dashed lines represent atmospheric *p*CO₂ value of 370 μatm.

Despite variation, a strong cross-system seasonal pattern was characterized by CO₂ evasion during spring and fall circulation, with uptake of atmospheric CO₂ prevalent during summer stratification (Fig. 1). This pattern is well-illustrated using box plots showing weekly cross-system variation (Fig. 1a) and weekly averages of *p*CO₂ across the 15 reservoirs against surface temperature (Fig. 1b). Samples were initially collected during the transition from ice cover to open water (first 8 weeks); during this period saturation steadily increased, with mean *p*CO₂ values nearly doubling from 310 to 610 μatm (Fig. 1).

All reservoirs were ice-free at week 9, and all *p*CO₂ values exceeded atmospheric equilibrium (average 634 μatm; Fig. 1). This period of increasing saturation includes loss of CO₂ resulting from metabolic activity under the ice (Pacheco et al. 2013, Ducharme-Riel et al. 2015).

A spring bloom interposed the cross-system pattern during the ensuing weeks (weeks 9–12), as measured by sharp increases in Chl-*a*_N (where N represents normalized values; Fig. 2), with *p*CO₂ declining to about two-thirds of the previous peak, presumably the consequence of biological production. Spring warming was reversed in mid-April (week 14; Fig. 1b); surface temperatures cooled by >1 °C, and all *p*CO₂ values exceeded atmospheric equilibrium (from 445 to 1048 μatm; Fig. 1a), averaging 654 μatm compared with 355 μatm the previous week. A clear-water phase coincided with this cooling event; Chl-*a*_N (Fig. 2) declined to among the lowest values measured during the study, and Chl-*a*:TP ratios decreased from >0.4 to ~0.25. The mean number of Cladocerans increased by nearly 50% from the previous week (from 29 to 57 individ. L⁻¹), suggesting grazing was a factor in suppressing algal biomass. The clear-water event persisted

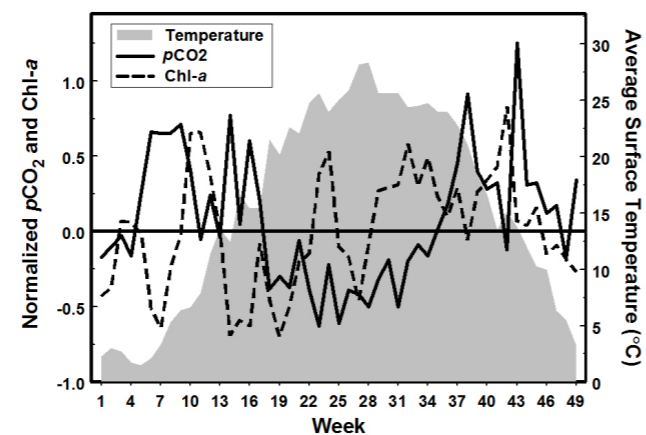


Fig. 2. Seasonal patterns of mean *p*CO₂ and Chl-*a* (both normalized using reservoir-specific mean and standard deviation information) and surface temperature in 15 north Missouri reservoirs sampled over a 49 week between 12 January and 15 December 2004. Vertical dashed lines represent seasonal cutpoints, with the vertical dotted line indicating ice-out.

Table 3. CO₂ flux (g m⁻² C) in 15 Missouri reservoirs for different time periods during the 49 weeks (wks) between 12 January and 15 December 2004.

Lake	Annual Flux (wks 1–49)	Open water (wks 9–49)	Spring (wks 1–17)	Summer (wks 18–35)	Fall (wks 36–49)
Nehai Tonkayea	8.0	9.2	1.3	-4.1	10.7
Forest	31.1	28.8	11.0	2.9	17.2
New Bethany	17.8	14.3	6.7	-1.3	12.3
Marie	7.0	7.0	9.5	-7.1	4.6
Brookfield	16.3	12.1	7.7	-4.0	12.5
Hazel Creek	13.4	10.7	7.8	-3.7	9.3
Marceline 2	15.9	18.4	-0.5	0.9	15.5
Green City	9.3	0.9	11.6	1.1	-3.3
Mozingo	27.7	21.6	15.4	-1.1	13.4
Harrison Co.	32.2	26.1	19.6	-4.4	17.0
Bilby Ranch	4.4	11.7	1.2	-8.6	11.8
Paho	1.5	-3.5	9.7	-5.7	-2.5
Nodaway	9.8	7.5	8.8	-7.1	8.1
Marceline 1	7.4	-3.5	10.7	-6.7	3.4
Sterling Price	-6.7	-14.3	12.6	-17.6	-1.7
Mean	13.0	9.8	8.9	-4.4	8.5
Median	9.8	10.7	9.5	-4.1	10.7

for about 1 month, and during this period some 80% of *p*CO₂ values exceeded atmospheric equilibrium ($n = 60$, mean 509 μatm; Fig. 1a).

Surface temperatures first reached >20 °C in mid-May (week 18), an increase of about 6 °C from the previous measure (Fig. 1b). Reservoirs in this region typically stratify about this time, and oxygen rapidly depletes in the hypolimnion, even in the least productive systems (Jones et al. 2011). During summer stratification, ~70% of *p*CO₂ measurements were below atmospheric equilibrium, averaging 66% of saturation (297 μatm, $n = 270$; Fig. 1). Undersaturation was measured in individual reservoirs in 39% (Forest) to 100% (Sterling Price) of summer samples, but only during a mid-June collection (week 23) were all weekly samples below atmospheric equilibrium (averaging 37%; Fig. 1); this collection coincided with a cross-system peak in Chl-*a*_N (Fig. 2). During summer stratification (weeks 18–35), mean *p*CO₂ was below saturation in 12 of 15 reservoirs (Table 3). These data support the finding of Balmer and Downing (2011) that, during summer, lakes in this region are largely undersaturated with CO₂.

Supersaturation dominated the cross-system pattern as temperatures declined and the mixed layer deepened with onset of fall destratification (Fig. 1). During mid-September through mid-October, the surface layer cooled ~10 °C; *p*CO₂ in 80% of these samples ($n = 90$),

exceeded equilibrium by 1.4-fold on average. Surface temperatures warmed by 1.5 °C in late October (week 42), resulting in ephemeral stratification. The cross-system pattern suggests a fall bloom occurred during this warming event; Chl-*a*_N spiked in these samples (Fig. 2), and *p*CO₂ averaged 365 μatm ($n = 15$), with more than half of the samples below equilibrium. The following week destratification continued; *p*CO₂ averaged 869 μatm, with all samples exceeding equilibrium (Fig. 1). This sequence demonstrates the role of physical processes (warming and cooling) on the lacustrine carbon budget as well as the dynamic nature of carbon fluxes at a regional scale. As the reservoirs attained full autumnal mixis, the mean *p*CO₂ value among the 90 samples collected in the final 6 weeks of the study was 481 μatm, and 70% were greater than equilibrium (Fig. 1).

Weekly estimates of *p*CO₂ flux were used to calculate seasonal and annual CO₂ budgets for the 15 reservoirs (Table 3). Net annual CO₂ flux varied from -6.7 to 32.2 g m⁻² yr⁻¹ C among these reservoirs (Table 3), with a mean and median of 13.0 and 9.8 g m⁻² yr⁻¹ C, respectively. Some 76% of variance in the cross-system range in net annual CO₂ flux was described by mean depth and flushing rate_(log) (positive coefficients; equation 1, Table 4), and these 2 metrics are inversely correlated among these reservoirs ($r = -0.79$). This model is consistent with earlier findings that morphology and hydrology determine reservoir trophic

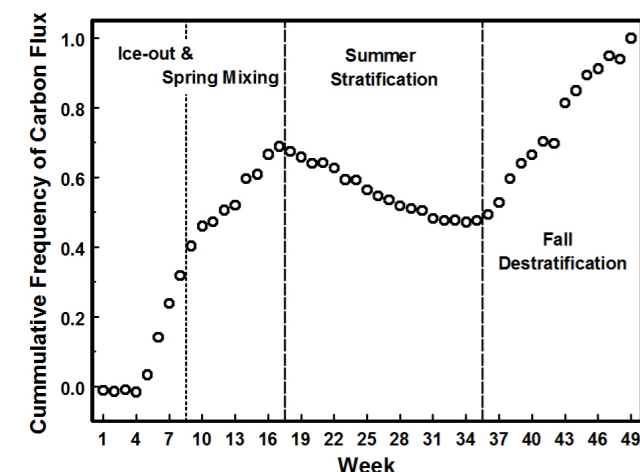
Table 4. Regression equations for CO₂ flux during 4 different time periods (AICc is the score for Akaike information criterion for small samples).

Flux Period	Equation	r ²	AICc
Annual	-34.2 + 97.9 (log mean depth) + 29.1 (log flushing rate)	0.76	61.4
Open Water	-42.3 + 104.5 (log mean depth) + 24.7 (log flushing rate)	0.89	51.9
Summer	-35.3 - 0.3 (Chl- <i>a</i>) + 29.1 (log DOC) + 3.7 (log volume)	0.81	38.5
Fall	-19.9 + 57.1 (log mean depth) + 13.5 (log flushing rate)	0.75	48.5

state (Jones et al. 2008a), and that these easily measured metrics provide a preliminary basis for estimating the role of impoundments in the regional carbon budget. These 2 variables were also significant when the negative flux value from Sterling Price was excluded from the analysis ($r^2 = 0.68$, model not shown, $n = 14$), demonstrating that the observed relationship was not biased by the sole net heterotrophic reservoir. DOC, a strong correlate of flushing rate ($r = 0.85$), could be substituted in the regression model with mean depth with a similar result ($r^2 = 0.68$, model not shown). This result is consistent with previous studies reporting $p\text{CO}_2$ increases with DOC (del Giorgio et al. 1999, Pace et al. 2004, Ducharme-Riel et al. 2015).

Cross-system correlations between annual CO₂ flux with mean values of the plant nutrients or measures of the organic base, however, were not significant. Average DO saturation varied from 77 to 86% in the 14 reservoirs with net CO₂ evasion and was 93% in Sterling Price, where net annual CO₂ uptake was measured. This finding generally agrees with Pacheco et al. (2013) that lakes with oxygen >95% saturation show CO₂ uptake.

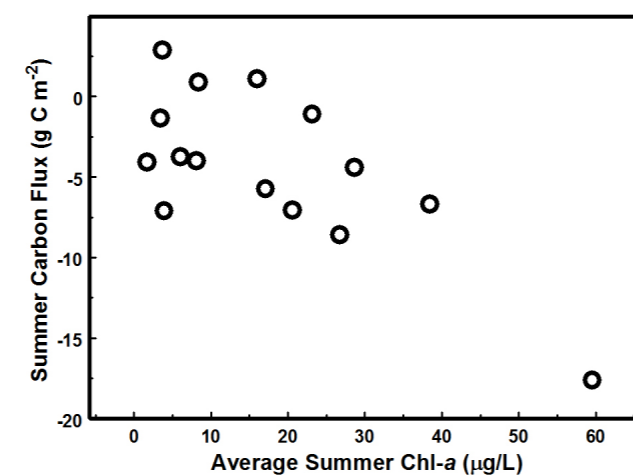
Net carbon flux during the open-water period (weeks 9–49, $n = 41$) was strongly correlated with net annual flux ($r = 0.92$, $n = 49$). Although the range and measures of central tendency for the 2 periods were similar (Table 3), the open-water period included 4 reservoirs with net flux

**Fig. 3.** Cumulative frequency distribution (running total) of carbon flux averaged by week across 15 north Missouri reservoirs sampled between 12 January and 15 December 2004.

values <1 g m⁻² C compared to only one for the annual period (Table 3). Similar to annual flux, ~89% of cross-system variation in open-water flux estimate (weeks 9–49) was accounted for by mean depth_(log) and flushing rate_(log) (positive coefficients; equation 2, Table 4). Also, DOC could be used with mean depth_(log) (positive coefficients, model not shown) to account for 86% of variation. This comparison shows strong correspondence between processes driving cross-system CO₂ flux annually and during the open-water period.

Depicting flux as an average cumulative sum over time (Fig. 3) illustrates a strong seasonal pattern of carbon release and uptake from these reservoirs. Some 70% of annual carbon efflux occurred by the end of spring mixis; during this period net flux was positive in all but one reservoir, ranging between -0.5 and 19.6 g m⁻² C (17 weeks), with an average of 8.9 g m⁻² C (Table 3). These flux values were negatively correlated with mean percent DO in surface samples ($r = -0.67$, $n = 15$), similar to regional findings (Balmer and Downing 2011, Pacheco et al. 2013).

During summer stratification (18 weeks), net CO₂ flux was negative in 12 of 15 reservoirs, with values ranging from -17.6 to 2.9 g m⁻² C and a mean of -4.4 g m⁻² C

**Fig. 4.** Average summertime carbon flux (g m⁻² C) for 15 northern Missouri reservoirs versus (a) average summer Chl-*a*. The lowest carbon flux and highest Chl-*a*, was measured in Sterling Price Reservoir. Negative values represent carbon uptake from the atmosphere by lake water.

(Table 3). Some 81% of cross-system variation in summer flux was explained by Chl-*a* (negative coefficient; Fig. 4), DOC_(log), and reservoir volume_(log) (both with positive coefficients; equation 3, Table 4). This relationship was not significant, however, when the most negative flux value (Sterling Price; Table 3) associated with a Chl-*a* value ~50% larger than the next highest value (60 vs. 38 µg L⁻¹, respectively; Fig. 4) was excluded. Numerous reservoirs in Missouri support summer Chl-*a* within this gap (Jones et al. 2008b), however, and additional research on carbon flux would help determine factors that account for the cross-system pattern during summer stratification. CO₂ evasion during summer was also negatively correlated with mean percent DO ($r = -0.78$), driven by a >100% value in Sterling Price. Atmospheric uptake of carbon during summer caused the mean cumulative sum value to decline by ~30% relative to the spring peak, such that by end of summer cumulative flux averaged ~50% of total annual flux (Fig. 3).

Subsequently, close to half of net annual efflux occurred during fall de-stratification (Fig. 3). The average during this 14 week season was 8.5 g m⁻² C, ranging from -3.3 to 17.2 g m⁻² C, with 12 of 15 reservoirs showing positive values (Table 3). Some 75% of variation in CO₂ flux during fall was explained by mean depth_(log) and flushing rate_(log) (positive coefficients; equation 4, Table 4), but DOC could be substituted for flushing rate with similar results ($r^2 = 0.73$, model not shown). Hypolimnetic decomposition during summer stratification, resulting in CO₂ accumulation, plays an important role in lake carbon budgets (Kortelainen et al. 2006, Urabe et al. 2011, Ducharme-Riel et al. 2015). During the breakdown of thermal stratification in these reservoirs, average percent DO in bottom samples increased from ~1% of saturation to >90%, coinciding with CO₂ evasion to the atmosphere. Flux during fall de-stratification was strongly correlated with annual flux ($r = 0.78$) and open-water flux ($r = 0.91$).

Discussion

Carbon uptake and evasion showed a strong seasonal pattern in these reservoirs (Fig. 1–3), with a prevalence of summer CO₂ uptake counterbalanced by efflux during other seasons (Fig. 3, Table 3). These net annual CO₂ flux values broadly fit within the lower range reported for temperate lakes worldwide and contribute to the growing database on CO₂ in mid-continent reservoirs (table 2 in Pacheco et al. 2013, Ducharme-Riel et al. 2015). The single negative annual carbon value (Sterling Price; -6.7 g m⁻² yr⁻¹) closely matches annual carbon uptake measured in 4 eutrophic systems located in nearby Iowa (Pacheco et al. 2013; from -18 to -6 g m⁻² yr⁻¹). The 3

largest values in our study (27.7–32.2 g m⁻² yr⁻¹) approach rates reported from temperate reservoirs (38 g m⁻² yr⁻¹; Barros et al. 2011), forested reservoirs in Ohio (33.6 g m⁻² yr⁻¹; Knoll et al. 2013), Finnish lakes (42 g m⁻² yr⁻¹; Kortelainen et al. 2006), and northern lakes (44.6 g m⁻² yr⁻¹; Ducharme-Riel et al. 2015). These maximum carbon values, however, are less than half the averages reported in some temperate lakes (99 g m⁻² yr⁻¹; Marotta et al. 2009) and an order of magnitude less than carbon emission from Florida lakes (328 g m⁻² yr⁻¹; Lazzarino et al. 2009). The remaining 11 carbon values (1.5–17.8 g m⁻² yr⁻¹) are low relative to rates measured in most temperate lakes, but evasion rates from these reservoirs bracket the value measured in an eutrophic lake studied by Pacheco et al. (2013; Black Hawk Lake with 10 g m⁻² yr⁻¹), agricultural reservoirs in Ohio (11.5 g m⁻² yr⁻¹; Knoll et al. 2013), and the lowest value measured in a suite of northern lakes (13.6 g m⁻² yr⁻¹; Ducharme-Riel et al. 2015).

Unlike the highly eutrophic waterbodies studied by Pacheco et al. (2013), only one reservoir showed net atmospheric uptake over the annual cycle (Sterling Price); it had the highest Chl-*a* levels (Table 1, Fig. 4) and highest average oxygen saturation. The discrepancy may partly be attributable to differences in lake trophic state between the 2 studies. On average, these Missouri reservoirs had about one-third the TP and TN concentration (average 44 vs. 147 µg L⁻¹, and 850 vs. 2646 µg L⁻¹, respectively) and about one-fourth the Chl-*a* content (17.3 vs. 68.6 µg L⁻¹) of waterbodies analyzed by Pacheco et al. (2013). Studies show CO₂ evasion generally declines with increasing lake productivity (Barros et al. 2011, Trolle et al. 2012).

Loss of CO₂ from these impoundments to the atmosphere, however, was modest relative to annual burial rates of sediment organic carbon. The average CO₂ flux for these 15 reservoirs was ~6% of the carbon buried in 4 northern Missouri impoundments (183 to 279 g m⁻² yr⁻¹ C; Pittman et al. 2013), which matches findings of other studies in the region (Knoll et al. 2013, Pacheco et al. 2013).

Annual and seasonal carbon flux from these impoundments was best described by morphology and hydrology, which also determine reservoir trophic state (Table 4; Jones et al. 2008a). These straightforward metrics provide the basis for estimating carbon uptake and evasion from regional reservoirs. The most undersaturated samples in our dataset came from the smallest reservoirs, which were the most rich in plant nutrients and algal biomass (Table 1 and 2). Regionally, impoundments with these characteristics can be expected to demonstrate conditions leading to uptake of atmospheric carbon. Globally, these results suggest that understanding and quantifying the carbon role of eutrophic lakes, especially small ones, have important implications for global carbon budgets and climate change.

Acknowledgements

This paper is dedicated to our friend Val Smith in recognition of his many contributions to limnology. Data were acquired with the support of the Missouri Department of Natural Resources, Missouri Agricultural Experiment Station and Food & Agriculture Policy Research Institute, and others. Any use of trade, product, or firm names is for descriptive purposes only and does not imply endorsement by the US Government.

References

- Balmer MB, Downing JA. 2011. Carbon dioxide concentrations in eutrophic lakes: undersaturation implies atmospheric uptake. *Inland Waters*. 1:125–132.
- Barros N, Cole JJ, Tranvik LJ, Prairie YT, Bastviken D, Huszar VLM, del Giorgio P, Roland F. 2011. Carbon emission from hydroelectric reservoirs linked to reservoir age and latitude. *Nat Geosci*. 4:593–596.
- Brown GS. 1979. Estimation of surface wind speeds using satellite-borne radar measurements at normal incidence. *J Geophys Res*. 84:3974–3978.
- Butler JN. 1992. Carbon dioxide equilibrium and their applications. Chelsea (MI): Lewis.
- Cole JJ, Caraco NF, Kling GW, Kratz TK. 1994. Carbon dioxide supersaturation in the surface waters of lakes. *Science*. 265:1568–1570.
- Cole JJ, Caraco NF. 1998. Atmospheric exchange of carbon dioxide in a low-wind oligotrophic lake measured by the addition of SF₆. *Limnol Oceanogr*. 43:647–656.
- del Giorgio PA, Cole JJ, Caraco NF, Peters RH. 1999. Linking planktonic biomass and metabolism to net gas fluxes in northern temperate lakes. *Ecology*. 80:1422–1431.
- Duarte CM, Prairie YT. 2005. Prevalence of heterotrophy and atmospheric CO₂ emissions from aquatic ecosystems. *Ecosystems*. 8:862–870.
- Ducharme-Riel VD, Vachon D, del Giorgio PA, Prairie YT. 2015. The relative contribution of winter under-ice and summer hypolimnetic CO₂ accumulation to the annual CO₂ emissions from northern lakes. *Ecosystems*. 18:547–559.
- Havel JE, Graham JL. 2006. Complementary population dynamics of exotic and native *Daphnia* in North American reservoir communities. *Arch Hydrobiol*. 167:245–264.
- Jones JR, Knowlton MF, Obrecht DO. 2008a. Role of land cover and hydrology in determining nutrients in mid-continent reservoirs: implications for nutrient criteria and management. *Lake Reserv Manage*. 24:1–9.
- Jones JR, Knowlton MF, Obrecht DV, Graham JL. 2011. Temperature and oxygen in Missouri reservoirs. *Lake Reserv Manage*. 27:173–182.
- Jones JR, Obrecht DV, Perkins BD, Knowlton MF, Thorpe AP, Watanabe S, Bacon RR. 2008b. Nutrients, seston and transparency of Missouri reservoirs and oxbow lakes: an analysis of regional limnology. *Lake Reserv Manage*. 24:155–180.
- Jonsson A, Åberg J, Jansson M. 2007. Variations in pCO₂ during summer in the surface water of an unproductive lake in northern Sweden. *Tellus B*. 59:797–803.
- Kling GW, Kipphut GW, Miller MC. 1992. The flux of CO₂ and CH₄ from lakes and rivers in arctic Alaska. *Hydrobiologia*. 240:23–36.
- Knoll LB, Vanni MJ, Renwick WH, Dittman EK, Gephart JA. 2013. Temperate reservoirs are large carbon sinks and small CO₂ sources: results from high-resolution carbon budgets. *Global Biogeochem Cy*. 27:52–64.
- Kortelainen P, Rantakari M, Huttunen J, Mattsson T, Alm J, Jutinen S, Larmola T, Silvola J, Martikainen PJ. 2006. Sediment respiration and lake trophic state are important predictors of large CO₂ evasion from small boreal lakes. *Global Change Biol*. 12:1554–1567.
- Lazzarino JK, Bachmann RW, Hoyer MV, Canfield DE. 2009. Carbon dioxide supersaturation in Florida lakes. *Hydrobiologia*. 627:169–180.
- Marotta H, Duarte CM, Sobek S, Enrich-Prast A. 2009. Large CO₂ disequilibria in tropical lakes. *Global Biogeochem Cy*. 23:GB4022. doi:10.1029/2008GB003434
- Pace ML, Cole JJ, Carpenter SR, Hodgon JR. 2004. Whole-lake carbon-13 additions reveal terrestrial support of aquatic food webs. *Nature*. 423:240–243.
- Pacheco FS, Roland F, Downing JA. 2013. Eutrophication reverses whole-lake carbon budgets. *Inland Waters*. 4:41–48.
- Pittman B, Jones JR, Millsbaugh JJ, Kremer RJ, Downing JA. 2013. Sediment organic carbon distribution in 4 small northern Missouri impoundments: implications for sampling carbon sequestration. *Inland Waters*. 3:39–46.
- Prairie YT, Bird DF, Cole JJ. 2002. The summer metabolic balance in the epilimnion of southeastern Quebec lakes. *Limnol Oceanogr*. 47:316–321.
- Raymond PA, Hartmann J, Lauerwald R, Sobek S, McDonald C, Hoover M, Butman D, Striegl R, Mayorga E, Humborg C, et al. 2013. Global carbon dioxide emissions from inland waters. *Nature*. 503:355–359.
- Sugiura N. 1978. Further analysis of the data by Akaike's information criterion and the finite corrections. *Comm Stat Theor Meth*. 7:13–26.
- Trolle D, Staehr PA, Davidson TA, Bjerring R, Lauridsen TL, Sondergaard M, Jeppesen E. 2012. Seasonal dynamics of CO₂ flux across the surface of shallow temperate lakes. *Ecosystems*. 15:336–347.
- Urabe J, Iwata T, Yagami Y, Kato E, Suzuki T, Hino S, Ban S. 2011. Within-lake and watershed determinants of carbon dioxide in surface water: a comparative analysis of a variety of lakes in the Japanese islands. *Limnol Oceanogr*. 56:49–60.